Human receptive endometrial organoid for deciphering the implantation window

Yu Zhang[acdef*], Rusong Zhao[abcdefgh*], Chaoyan Yang[acdef], Jinzhu Song[acdef], Peishu Liu[i], Yan Li[acdefgh], Boyang Liu[acdefgh], Tao Li[jk], Changjian Yin[acdef], Minghui Lu[acdef], Zhenzhen Hou[acdef], Chuanxin Zhang[acdef], Zi-Jiang Chen[acdefghlm#], Keliang Wu[acdefgh#], Han Zhao[acdefgh#]

Author affiliation:

a. State Key Laboratory of Reproductive Medicine and Offspring Health, Center for Reproductive Medicine, Institute of Women, Children and Reproductive Health, Cheeloo College of Medicine, Shandong University, 250012, China

b. The Affiliated Suzhou Hospital of Nanjing Medical University, Suzhou Municipal Hospital, Gusu School, Nanjing Medical University, Suzhou, Jiangsu, 215000, China

c. National Research Center for Assisted Reproductive Technology and Reproductive Genetics, Shandong University, Jinan, Shandong, 250012, China

d. Key Laboratory of Reproductive Endocrinology (Shandong University), Ministry of Education, Jinan, Shandong, 250012, China

e. Shandong Technology Innovation Center for Reproductive Health, Jinan, Shandong, 250012, China

f. Shandong Provincial Clinical Research Center for Reproductive Health, Jinan, Shandong, 250012, China

g. Shandong Key Laboratory of Reproductive Medicine, Shandong Provincial Hospital Affiliated to Shandong First Medical University, Jinan, Shandong, 250012, China

h. Research Unit of Gametogenesis and Health of ART-Offspring, Chinese Academy of Medical Sciences (No.2021RU001), Jinan, Shandong, 250012, China

i. Department of Obstetrics and Gynecology, Qilu Hospital of Shandong University, Jinan, Shandong, 250012, China

j. Department of Gynecology, Shandong Provincial Hospital, Cheeloo College of Medicine, Shandong University, Jinan, Shandong, 250021, China.

k. Department of Gynecology, Shandong Provincial Hospital Affiliated to Shandong First Medical University, Jinan, Shandong, 250021, China

l. Shanghai Key Laboratory for Assisted Reproduction and Reproductive Genetics, Shanghai, 200135, China

m. Department of Reproductive Medicine, Ren Ji Hospital, Shanghai Jiao Tong University School of Medicine, Shanghai, 200135, China

*These authors contributed equally: Yu Zhang, Rusong Zhao.

[#]To whom correspondence may be addressed. Email: hanzh80@sdu.edu.cn, wukeliang_527@163.com, chenzijiang@hotmail.com

Classifications: Cell Biology

Abstract

Human endometrial receptivity is a critical determinant of pregnancy success; however, in vivo studies of its features and regulation are particularly challenging due to ethical restriction. Recently, the development of human endometrial organoids has provided a powerful model to examine this intricate biological process. In this study, we established a specialized human window-of-implantation (WOI) endometrial organoid system that mimics the in vivo receptive endometrium. The endometrial organoid recapitulates not only the structural attributes of glands and stroma, but also the in vivo endometrium's cell types at the single-cell level. Furthermore, the WOI endometrial organoid exhibits the features of in vivo implantation endometrium such as hormone responsiveness, secretory functions, and distinctive implantation window hallmarks, including decidualization, extracellular matrix (ECM) remodeling, pinopode formation, cilia generation and metabolism. This in vitro model also effectively demonstrates the process of proliferation-secretory transformation, ciliary epithelium differentiation, and epithelial-mesenchymal transition (EMT). As such, WOI organoids hold great promise as an alternative platform to unravel the intricate mechanisms governing endometrial receptivity regulation, maternal-fetal interactions, and associated diseases, ultimately driving impactful advancements in the field.

Keywords

Endometrium, organoid, implantation window

Introduction

The human endometrium, comprising various cell types, experiences shedding (menstrual phase), regeneration (proliferative phase), and differentiation (secretory phase) under the regulation of estrogen and progesterone during the menstrual cycle (1). A brief window, called the "window-of-implantation (WOI)" or mid-secretory phase, allows for embryo implantation into the endometrium (1). The endometrium at the embryo implantation site contains diverse cells, including ciliated epithelial cells, decidualized stromal cells and immune cells. Cyclic endometrial changes akin to those in humans are exclusive to apes, Old World monkeys, molossid bats, and spiny mice, but not mice (1), rendering typical mouse models insufficient for accurately simulating human endometrium. Existing endometrial cell lines, such as Ishikawa and HEEC cells, consist solely of a single cell type, thus failing to reproduce the intricate physiological structure and function of the endometrium.

Replicating and reconstructing human organs has become essential for exploring tissue physiology and function. Organoid, a self-assembled 3D structure, closely resemble in vivo tissue or organ (2). They offer high expansibility, phenotypic, and functional properties, emerging as powerful tools for investigating tissue physiology and disease (3). In 2017, the first long-term and hormone-responsive human endometrial organoid was established using adult stem cells from endometrial biopsy(2). Based on this, Margherita Y. Turco, et al developed noninvasive methods to construct endometrial organoids from menstrual flow(4). Apart from adult stem cells, pluripotent stem cells were also induced to endometrial stromal fibroblasts and epithelium, and then cocultured to form organoids(5, 6), which offered vigorous proliferative capacity but lacked immune cells and other components of the microenvironment. There are also studies that add immune cells to endometrial organoids for co-culture(7). In efforts to mimic human endometrial cell types in vitro, the endometrial organoids progressed from epithelial organoids(8), to assemblies of epithelial and stromal cells(9, 10) and then to stem cell-laden 3D artificial endometrium(11, 12), which were solely closer but not completely identical to the endometrium. Additionally, pathological endometrial organoid models have been established for conditions like endometriosis, endometrial hyperplasia, Lynch syndrome, and endometrial cancer (13). These organoids simulated endometrial morphology, hormone responsiveness, and physiological and pathological processes

in vitro (3, 8, 14-16), facilitating the study of physiological phenomena (14, 17, 18), pathogenic mechanisms(15) and drug screening(13).

Although various regulators have been suggested to be involved in WOI, we are far from understanding how embryo implantation occurs during the WOI due to ethical limitations and fewer in vitro receptive endometrial model. Transforming from proliferative to receptive endometrium involves dynamic changes like decidualization, epithelial-mesenchymal transition (EMT) and ciliated epithelial development (1, 19), which have not been reconstructed in most in vitro model to date. Here, we successfully established a receptive endometrial organoid system regulated by hormones and reflecting the in vivo WOI endometrial features, providing a platform for studying physiological and pathological endometrium and maternal-fetal interactions.

Results

Endometrial organoids possess endometrial morphology and function

To establish endometrial organoids in vitro, pre-receptive endometrium from reproductive-age women was dissociated into single cells or small cell masses. These cells then self-assembled into organoids induced by various small molecules, such as Noggin, EGF, FGF2, WNT-3A and R-Spondin1 in expansion medium (ExM) (Fig.1A). The endometrial organoids consist of vesicle-like glands, fibrous stromal cells, and other surrounding cells, and they were capable of being passaged (Fig. 1B~1C, Fig. S1A~S1B, Video S1~S4). As the organoids grew and differentiated, the endometrial glands enlarged, epithelial cells adopted a paving stone arrangement, and stromal cells formed an extensive network (Fig. 1C). The epithelium marker E-cadherin, stromal cell marker vimentin, and endometrial gland marker FOXA2 were expressed in the cultured endometrial organoid, which resembled the endometrium morphologically (Fig. 1D). Moreover, the endometrial organoids exhibited substantial expression of the proliferation marker Ki67, while the apoptosis marker cleaved caspase-3 was undetectable, signifying the organoids' robust proliferative capacity (Fig. 1E).

Functionally, endometrial organoids effectively secreted glycogen into the lumen, mirroring the in vivo endometrial activity, thereby providing nourishment for embryo implantation (Fig. 1D). Moreover, after treatment with estrogen (E2) for two days followed by administration of medroxyprogesterone acetate (MPA) and cAMP for fourteen days, the organoids exhibited a notable upregulation of progesterone receptor (PR A/B) expression and a modest increase in estrogen receptor α (ERα) compared to the control group (Fig. S1C~S1D). It reflected a comparable hormonal responsiveness in the in vivo endometrium.

To identify hormonal regimens that induce implantation window, pregnancy-related hormones were supplemented into the culture system following the two-day E2. E2 and MPA promote the transition of endometrial organoids into the secretory phase, while pregnancy hormones can promote the further differentiation. Prolactin (PRL) promotes immune regulation and angiogenesis during implantation(2, 20). Human chorionic gonadotropin (hCG) improves endometrial thickness and receptivity (21, 22). Human placental lactogen (hPL) promotes the development and function of endometrial glands(23). Hormone dosage was primarily based on peri-pregnant maternal body

or localized endometrium levels (2). A comparison of multiple groups revealed similar counts, area, and average intensity of organoids over time (Fig.S1E). However, only the final recipe (i.e. a combination of E2, MPA, cAMP, PRL, hCG and hPL) exhibited an endometrial receptivity-related gene expression profile, which highly expressed genes positively correlated with endometrial receptivity, and lowly expressed genes negatively correlated with receptivity, compared to the other hormone formulations (Fig.S1F). The organoids induced with this scheme were defined as WOI organoids (Fig. 1A). In contrast, endometrial organoids maintained in ExM constituted the "control (CTRL)" group, whereas organoids treated with E2 for two days, followed by E2, MPA, and cAMP for an additional six days, were induced to the secretory phase as previously reported(8), and designated as the "secretory (SEC)" group (Fig. 1A). Theoretically, the WOI organoids are initially in the secretory phase, thus sharing characteristics with the SEC organoids. More importantly, they are expected to display traits typical of the mid-secretory phase. There was no significant difference in the morphology of organoids among the three groups (Fig.1B). The glycogen secretion of CTRL, SEC and WOI organoids showed an increasing trend (Fig.S1G).

Developing receptive endometrial organoids in vitro mimicking the implantation-window endometrium

Single-cell transcriptomics analysis identified the presence of epithelium, stromal cells, and immune cells in WOI organoids with reference to CellMarker, PanglaoDB, Human Cell Atlas, Human Cell Landscape, and scRNASeqDB, and previous endometrium related studies(1, 8, 10, 24) (Fig. 2A, Fig. S2A~S2B). The WOI organoids exhibited similarities to the mid-secretory endometrium in terms of glandular and luminal epithelium, secretory epithelium, LGR5 epithelium, ciliated epithelium, and EMT-derived stromal cells, as evidenced by comparisons of scRNA-seq data from our organoids and the mid-secretory endometrium as described by Stephen R. Quake in 2020 (1) (Fig.2A, Fig.S2C~S2D). The morphology of immune and stromal cells was analyzed through 3D clearing staining and light sheet microscopy imaging, with vimentin labeling stromal cells, CD45 and CD44 indicating immune cells, and FOXA2 identifying glands (Fig.2B~2C). Furtherly, we confirmed the presence of immune cells and investigated the proportion of T cells and macrophages using flow cytometry. White blood cells (WBC) were identified as $CD45^{+}$ cells, with T cells and

macrophages characterized as $CD45^+CD3^+$ cells and $CD45^+CD68^+CD11b^+$ cells, respectively (Fig. 2D). The proportion of WBC in organoids was approximately 3%~4% (Fig.2D), among which macrophages were less than 1% and T cells less than 2% (Fig. S2E). The percentage of WBCs in WOI organoids was lower than that in CTRL organoids, among which T cells decreased in the WOI organoids (Fig. S2F).

Our study concentrated on the comparison of gene expression and transcriptional regulation during the mid-secretory phase, as this phase marks the implantation window and involves substantial transcriptional alterations (Fig.2E~2F). We referred to the scRNA-seq data of the mid-secretory phase from Stephen R. Quake 2020 (1). Pathways related to mitochondrial energy metabolism, cell adhesion, cytoskeleton regulation, and epithelial cell growth exhibited upregulation in both the WOI organoid and mid-secretory endometrium in comparison to the CTRL and SEC organoids (Fig. 2E). The crucial transcription factors (TFs) found in the secretory epithelium and EMT-derived stromal cells, which are implicated in implantation, revealed similarities between WOI organoids and mid-secretory endometrium. Specifically, the secretory epithelium exhibited comparable TFs related to hypoxia response (such as previously reported HIF1A(25)), embryo implantation (such as FBLN1(26)), lipid metabolism (such as VMP1(27)), cell migration, and cell junction (such as TJP1(28)) (Fig. 2F). Similarly, EMT-derived stromal cells also expressed similar TFs involved in endometrial decidualization (such as S100A10(29)), EMT (such as FAT1(30) and FOXF2(31)), and receptivity (such as NEAT1(32), SERPINB9(33), SOX17(34) and SOX4(35)) (Fig. 2F).

We then conducted the endometrial receptivity test (ERT) (36) and explored microstructure to further assess the receptive state of WOI organoids (Fig. 2G). ERT is a kind of gene analysis-based method for detecting endometrial receptivity, which combines high-throughput sequencing and machine learning to analyze the expression of endometrial receptivity-related genes (36). It is currently used in clinical practice to determine endometrial receptivity and guide personalized embryo transfer. The WOI organoids derived from pre-receptive endometrium were observed to transit into the receptivity phase (Fig. 2G). Besides, the WOI organoids possessed various characteristic microstructure of implantation window, including elongated microvilli and increased glycogen, pinopodes, and especially cilia (Fig.2H).

Collectively, these results demonstrated that the WOI organoids closely resemble the in vivo

endometrium during the implantation window in terms of cell composition, function, transcriptional regulation, and endometrial receptivity.

Receptive endometrial organoids recapitulate WOI-associated biological characteristics

We analyzed the transcriptome and proteome profiles of WOI organoids compared to those of CTRL or SEC organoids to assess WOI associated biological characteristics (Fig. 3A, 3E, Fig. S3A~S3D). WOI organoids exhibited a robust hormone response, as demonstrated by the upregulation of PGR at the transcriptome level (Fig. 3B). Integrated analysis of the transcriptome and proteome data identified 179 upregulated genes/proteins in WOI organoids compared to the CTRL group (Fig. S3E), with most of these genes/proteins implicated in the estrogen response (Fig. S3F). Furthermore, the analysis of progesterone response levels using PRA/B immunostaining indicated the highest levels in the WOI group, accompanied by an upregulation of the estrogen responsive protein OLFM4 (Fig. 3C). FOXO1, a crucial marker of endometrial receptivity reliant on PGR signaling, exhibited significantly elevated expression in WOI organoids compared to CTRL organoids (Fig.3D, Video S5), suggesting the involvement of progesterone signaling in the establishment of WOI organoids. These findings collectively demonstrated a strong response of WOI organoids to estrogen and progesterone.

The growth and development, assembly and movement of cilia, a characteristic endometrial structure, are essential for the establishment of endometrial implantation window and embryo implantation. Cilia assembly(marked by acetyl-α-tubulin(14)) and motile cilia (marked by TPPP3 and ODF2(37)) were prominently observed in the WOI organoids (Fig. 3F~3G, Fig. S3I). Moreover, the expression of tubulin, integrin, and components of the PI3K-Akt pathway was also upregulated in the WOI organoids, which functioned to generate pinopodes, and respond to invasion (Fig. 3F, Fig. S3J). Under the electron microscopy, the cilia were most observed in the WOI organoids, while the pinopodes of WOI organoids exhibited the densest arrangement on the luminal side of epithelium among these three groups (Fig. 2H). These structures marked the establishment of endometrial receptivity and benefited for the embryo adhesion to the endometrium.

Other characteristics of the implantation window involved decreased cell proliferation (marked by CDH5 and MEIS1), increased cell differentiation (marked by FGFBP1 and TFF1), extracellular

matrix (ECM) remodeling (marked by PDGFB and IGFBP4(38)) and reduced cell adhesion (marked by EFNA5, LAMA3 and RHO GTPase) (Fig. 3B, Fig. S3G). Besides, energy metabolism (represented by SLC25A1(39)) and hypoxia response (represented by HIF1α(25)) were also characteristically enhanced in WOI organoids (Fig. 3B, Fig. S3F~S3H), which maintained the receptive state of endometrial organoids.

Overall, although the WOI organoids possessed the characteristics of implantation window, the differences in transcriptome and proteome between SEC and WOI organoids at the organoid level are not significant. This is understandable as WOI organoids are further induced towards the implantation window based on the secretory phase (i.e. SEC organoids), which prompted us to continue exploring at the single-cell level.

Structural cells construct WOI with functionally dynamic changes

Based on the WOI associated biological characteristics at the organoid level, we further examined the functionally dynamic changes in structural cells during the implantation window. The WOI organoids displayed more thoroughly differentiation to the mid-secretory endometrium than the SEC organoids at the single-cell level.

In terms of energy metabolism, the WOI organoids exhibited upregulation of monocarboxylic acid and lipid metabolism, and hypoxia response (Fig.3B, Fig.S3F). Likewise, the secretory epithelium, critical for the implantation window, contributed to cellular metabolic processes and HIF-1 signaling pathway response to hypoxia at the single-cell level (Fig. 4A, Fig. S2G). The secretory epithelium of WOI organoids exhibited enhanced peptide metabolism and mitochondrial energy metabolism compared to the SEC group, supporting endometrial decidualization and embryo implantation (Fig. 4B). Moreover, increased secretory epithelium and decreased proliferative epithelium in the SEC and WOI organoids suggested the transformation from proliferation to secretory phase (Fig. 4A). Proliferative epithelium differentiates into secretory epithelium under the regulation of branch nodal genes between state 5 and state 6, such as the GAS5, RPL and RPS families, as revealed by single-cell trajectory (Fig. 4C, Fig. S4A~B, Fig. S4G). The WOI organoids showed more thoroughly differentiation from proliferative to secretory epithelium in relation to the SEC organoids (Fig. 4C, Fig. S4A). Overall, the WOI organoids indicated more comprehensive differentiation to the

secretory epithelium with increased energy metabolism and hypoxia response during the implantation window.

Given that the WOI organoids exhibited increased cilia assembly and motile cilia, the transformation and function of the ciliated epithelium gained attention. Single-cell transcriptome analysis revealed hormone treatment increased ciliated epithelium and decreased unciliated epithelium in SEC and WOI groups by altering the expression of key genes, such as KRT19, MALAT1, RPL21 and RPS2 (Fig. 4A, 4D, Fig. S4C~D, Fig. S4H). Ciliated epithelium functioned in protein binding, cilium organization and assembly, while unciliated epithelium acted on actin cytoskeleton and translation (Fig. S2G). The WOI organoids' ciliated epithelium regulated vasculature development and displayed higher transcriptional activity than the SEC group (Fig. S2H). The implementation of these functions depended on its interaction with other cells. CellPhoneDB is a useful tool to investigate ligand-receptor interactions between the cells. Ciliated epithelium interacted with immune cells and secretory epithelium, modulating angiogenesis via NRP1-VEGFA and NRP2-VEGFA(40), with NRP2 highly expressed in the WOI organoids (Fig. 4F, Fig. S3K). Besides, the ciliated epithelium of WOI organoids showed enhanced invasion ability via CD74-COPA(41), and ROR2-WNT5A(42), which was validated by proximity ligation assay (PLA) (Fig. 4F, Fig. S2J). Thus, WOI organoids revealed accumulated ciliated epithelium's role in preparing the implantation window.

The WOI organoids displayed upregulated cell differentiation not only at organoid level but also at cellular level, which is represented by EMT. EMT is a common and crucial biological event in the endometrium during the implantation window(43). During the EMT process, epithelial cells lose their epithelial characteristics while gaining migratory and invasive properties of fibroblasts. Synthetic analysis of the transcriptome and proteome revealed increased EMT in WOI organoids (Fig. S3F). EMT-derived stromal cells, exhibiting gene expression patterns typical of epithelial and stromal cells, as well as EMT, are more abundant in the SEC and WOI groups, and act on protein binding, cell cycle, organelle organization, and reproduction (Fig. 4A, Fig. S2G). They performed enhanced lamellipodium-mediated cell migration, cell junction and cytoskeleton regulation in the WOI organoids compared to the SEC organoids (Fig. S2H). The WOI organoids exhibited more thoroughly differentiation from proliferative epithelium to EMT-derived stromal cells than the SEC

organoids, which was regulated by key genes such as DOC2B, FXYD3, and LPCAT3 (Fig. 4E, Fig. S4E~F, Fig. S4I). EMT-derived stromal cells and epithelium cooperated in transitioning from proliferation phase to implantation window (Fig.4G). We found that NRP1 and SLC7A1 were highly expressed by EMT-derived stromal cells, and their receptors (SEMA3A and CSF1) were more upregulated in the epithelium of WOI group than SEC group (Fig.4G, Fig. S2J). NRP1-SEMA3A has been reported to promote vascularization and responds to hypoxia(44). SLC7A1(45) and CSF1(46) both support receptivity establishment, embryo implantation and development. However, angiogenesis-related (NRP1-VEGFB and ADRB2-VEGFB), and TNF-related pathways were downregulated in WOI organoids (Fig.4G), which may link with pregnancy establishment and warrant further exploration (47). Compared with common stromal cells, EMT-derived stromal cells communicate slightly differently with epithelial or immune cells. CD44 and CD46, known for their roles in cell adhesion (48) and immunoregulation(49), are highly expressed in stromal cells and EMT-derived stromal cells, respectively, and bind separately with SPP1 and JAG1 in epithelial and stromal cells (Fig. 4G, Fig. S2I~S2J). In general, WOI organoids demonstrated EMT's role in mediating endometrial transformation towards the implantation window.

Discussion

In our study, we constructed the WOI endometrial organoids, and observed the remarkable resemblance in structure and function to the in vivo endometrium. The organoids consist of three primary types of endometrial cells, specifically epithelial, stromal, and immune cells, with epithelial cells assembling into glands and surrounded by immune cells and stromal cells. This similarity in cellular composition and tissue architecture to the endometrium lays the foundation for simulating receptive endometrium.

Although previous studies treated endometrial organoid with E2, P4, and cAMP to induce a transition to the secretory phase, the methodology to accurately simulate the implantation window or mid-secretory endometrium remains elusive and warrants further investigation. Previous research suggested that placental signals could further promote the differentiation of endometrial organoids (2), and PRL, hCG and HPL have been implicated in processes such as decidualization, implantation, immunoregulation, and angiogenesis (20, 21, 23). Detailly, PRL, synthesized by the adenohypophysis, endometrium, and myometrium, plays a vital role in implantation, immunoregulation, and angiogenesis, with the secretory endometrium producing PRL in response to MPA and E2, leading to ciliated cell formation and stromal cell decidualization (2, 20). HCG, secreted by trophoblasts in early pregnancy, influences decidual cells (21) and improves endometrial thickness and receptivity(22). The introduction of hCG has been shown to elevate the expression of critical factors associated with endometrial receptivity, such as endocytosis proteins, hypoxia-inducible factor 1 (HIF1), chemokines, and glycodelin (50). HPL contributes to the development and function of uterine glands(23). Consequently, the additional supplementation of PRL, hCG and HPL in our system augmented hormone responsiveness and receptivity, while promoting cell differentiation, ultimately yielding a model more representative of the receptive endometrium.

Here, our WOI organoids exhibit distinct characteristics resembling those of the in vivo receptive endometrium, including heightened energy and lipid metabolism. Enhanced energy metabolism involves monocarboxylic acid metabolism and mitochondrial oxidative phosphorylation. Monocarboxylic acids, exemplified by lactate, pyruvate, and ketone bodies, are vital metabolites in most mammalian cells. During the implantation window, elevated lactate levels mobilize

endometrial monocarboxylic acid metabolism and function as a pregnancy-related signal, stimulating secretion in the epithelium. Subsequently, ATP, the primary product of energy metabolism, induces neighboring epithelial cells to release IL8, promoting decidualization of stromal cells (51). It was also observed that WOI organoids indeed produced much more ATP and IL8 than CTRL and SEC organoids (Fig.S3L). Lipid metabolism, responsible for energy storage, signal transduction, cell proliferation, apoptosis, and membrane trafficking, plays a crucial role in endometrial receptivity and implantation, although the precise mechanisms are not fully understood (52-54). Thus, the WOI organoids possessed metabolic characteristics of in vivo implantation window.

Functional alterations in secretory epithelium and EMT-derived stromal cells at the single-cell level also occur during the implantation window and warrant further investigation. The secretory epithelium responds to hypoxia through the HIF1 signaling pathway during the implantation window. HIF1A maintains oxygen homeostasis by increasing VEGF levels throughout the menstrual cycle, while HIF2A promotes angiogenesis for embryo implantation (25, 55). Angiogenesis and vascular remodeling support functional endometrial layer repair, endometrial thickening, receptivity, and embryo implantation. Importantly, EMT, a signature transition to the receptive endometrium, occurs in the proliferative epithelium and EMT-derived stromal cells and facilitates opening the epithelial layer of endometrium(43), during which epithelial cells lose polarity and cell-to-cell junctions, stromal cells acquire the migratory and invasive abilities (56). These implantation window associated cellular characteristics are partly reproduced in the WOI organoids, which confirms that they are closer to the in vivo state. The WOI organoids will allow us to explore the underlying mechanisms and advance the field of embryo implantation research.

However, our WOI endometrial organoids also exhibit some limitations. Firstly, a decreased abundance of immune cells, particularly T cells expressing TSPYL2, RSRP1, and CD44, was observed in WOI organoids, indicating potential immunoregulation of embryo implantation. However, the composition of immune cells in organoids differs from that of the in vivo endometrium. Specifically, the proportion of WBCs in organoids was found to be lower than that in the

endometrium. Additionally, the proportions of T cells and macrophages in organoids were approximately 2% to 3% and 1% (Figure 2D), respectively, compared to 7% to 8% lymphocytes and 0.6% to 0.7% macrophages in the endometrium(1). Furthermore, during the implantation window, T cells in WOI organoids decreased (Figure S2F), while T cells in the endometrium increased(1). Secondly, it is undeniable that the organoids cannot perfectly replicate the in vivo endometrium, which comprises functional and basal layers with a greater abundance of cell subtypes, under superior regulation by systemic hormones and nutrients. Thirdly, the endometrial organoids lack the mechanical properties of the myometrium, which have an impact on the in vivo endometrium (57). We are looking forward to constructing the whole uterus in vitro with stem cell induction, 3D printing technology, and microfluidic systems.

In summary, we developed a receptive endometrial organoid that mimics the features of in vivo implantation-window endometrium (Fig. 5). Our human endometrial organoid comprises epithelial cells, stromal cells, and immune cells, ensuring hormone responsiveness and endometrial secretion function while recapitulating aspects such as decidualization, ECM remodeling, pinopode formation, cilia generation, EMT and metabolism. WOI organoids exhibit differentiation from SEC organoids towards the implantation window. The SEC organoids are suitable for studying endometrial secretory phase and hormone reactivity. This receptive endometrial organoid serves as a platform to investigate peri-implantation endometrial physiology and pathology, maternal-fetal interactions, with potential practical applications and clinical translation.

Materials and Methods

Establishment of endometrial organoids

All experiments involving human subjects followed medical ethical principles and the Declaration of Helsinki, and were approved by the Ethics Committee of Qilu Hospital of Shandong University. Informed consents were obtained from patients. Females of reproductive age who received hysterectomy for benign diseases were selected for this study. Clinical information of patients providing endometrial tissue was listed in Dataset S1. Experimental procedures are presented in detail in the Supporting Information.

Hormone treatment of endometrial organoids

The hormone regimen for inducing endometrial secretory phase, as described by Thomas E. Spencer et al (8), consisted of estradiol for 2 days followed by a combination of estradiol (Sigma E2758), medroxyprogesterone acetate (Selleck S2567) and N6,2′-O-dibutyryladenosine 3′,5′-cyclic monophosphate sodium salt (cAMP) (Sigma D0627) for 6 days.

To simulate the endometrium of implantation window, we developed a model by incorporating various pregnancy-related hormones. The hormone regimen included estradiol for the first two days, followed by a combination of estradiol, medroxyprogesterone acetate, cAMP, Human Chorionic Gonadotropin (HCG) (Livzon Pharmaceutical Group Inc), Human Placental Lactogen (HPL) (R&D Systems 5757-PL), and prolactin (Peprotech 100-07) for 6 days. The CTRL group was cultured in ExM without the addition of hormones. (Fig. 1A) (Table S2)

ACKNOWLEDGMENTS

This work was supported by National Natural Science Foundation of China (82192874 to H.Z), the National Key Research and Development Program of China (2021YFC2700301 to K.W), the Basic Science Center Program (31988101 to Z-J.C.), Fundamental Research Funds for the Central Universities(2022JC006 to K.W), the Fundamental Research Funds of Shandong University Taishan Scholars Program of Shandong Province（ts20190988 to H.Z.; tsqn201909194 to K.W）, Innovative research team of high-level local universities in Shanghai (SHSMU-ZLCX20210201 to

K.W).

We sincerely appreciate Prof. Tianqing Li (Kunming University of Science and Technology) and Prof. Shaorong Gao (Tongji University) for insightful comments and discussions.

We are grateful to Guangzhou Genedenovo Biotechnology Co., Ltd for assisting in sequencing and bioinformatics analysis. We also thank to YiKon Medical from China for technological assistance of ERT, Jingjie PTM Biolab (HangZhou) Co., Inc. for proteomics.

Author contributions: H. Zhao, K. Wu and Z.-J.C conceived the project and supervised research. Y. Zhang, R. Zhao and H. Zhao designed the experiments. Y. Zhang and R. Zhao performed the experiments, analyzed and interpreted data. Y. Zhang wrote the manuscript. R. Zhao, Y. Li, B. Liu, and H. Zhao revised the manuscript. P. Liu provided human endometrium samples. C.Yang, J. Song, T. Li, C. Yin, M. Lu, Z. Hou and C. Zhang provided technical support. All authors revised and approved the manuscript.

The authors declare no competing interest.

References

1. W. Wang *et al.*, Single-cell transcriptomic atlas of the human endometrium during the menstrual cycle. *Nat Med* **26**, 1644-1653 (2020).
2. M. Y. Turco *et al.*, Long-term, hormone-responsive organoid cultures of human endometrium in a chemically defined medium. *Nat Cell Biol* **19**, 568-577 (2017).
3. M. Boretto *et al.*, Development of organoids from mouse and human endometrium showing endometrial epithelium physiology and long-term expandability. (2017).
4. T. Cindrova-Davies *et al.*, Menstrual flow as a non-invasive source of endometrial organoids. *Commun Biol* **4**, 651 (2021).
5. V. C. Cheung *et al.*, Pluripotent stem cell-derived endometrial stromal fibroblasts in a cyclic, hormone-responsive, coculture model of human decidua. *Cell Rep* **35**, 109138 (2021).
6. L. Gong *et al.*, Bi-potential hPSC-derived Mullerian duct-like cells for full-thickness and functional endometrium regeneration. *NPJ Regen Med* **7**, 68 (2022).
7. L. Dolat, R. H. Valdivia, An endometrial organoid model of interactions between Chlamydia and epithelial and immune cells. *Journal of Cell Science* **134** (2021).
8. P. D. Harriet C. Fitzgerald, Susanta K. Behura, Danny J. Schust, and Thomas E. Spencer, Self-renewing endometrial epithelial organoids of the human uterus. *Proc Natl Acad Sci U S A*, 23132-23142 (2019).
9. T. Wiwatpanit *et al.*, Scaffold-Free Endometrial Organoids Respond to Excess Androgens Associated With Polycystic Ovarian Syndrome. *J Clin Endocrinol Metab* **105**, 769-780 (2020).
10. K. M. Thomas M Rawlings, Deborah M Taylor, Matteo A Molè, Katherine J Fishwick, Maria Tryfonos, Joshua Odendaal, Amelia Hawkes, Magdalena Zernicka-Goetz, Geraldine M Hartshorne, Jan J Brosens, Emma S Lucas, Modelling the impact of decidual senescence on embryo implantation in human endometrial assembloids. *eLife* **2021;10:e69603** (2021).
11. S. R. Park *et al.*, 3D stem cell-laden artificial endometrium: successful endometrial regeneration and pregnancy. *Biofabrication* **13** (2021).
12. S. R. Park *et al.*, Development of cell-laden multimodular Lego-like customizable endometrial tissue assembly for successful tissue regeneration. *Biomater Res* **27**, 33 (2023).
13. M. Boretto *et al.*, Patient-derived organoids from endometrial disease capture clinical heterogeneity and are amenable to drug screening. *Nat Cell Biol* **21**, 1041-1051 (2019).
14. S. Haider *et al.*, Estrogen Signaling Drives Ciliogenesis in Human Endometrial Organoids. *Endocrinology* **160**, 2282-2297 (2019).
15. D. R. Cochrane *et al.*, Single cell transcriptomes of normal endometrial derived organoids uncover novel cell type markers and cryptic differentiation of primary tumours. *J Pathol* **252**, 201-214 (2020).
16. B. N. Bui *et al.*, Organoids can be established reliably from cryopreserved biopsy catheter-derived endometrial tissue of infertile women. *Reprod Biomed Online* **41**, 465-473 (2020).
17. H. C. Fitzgerald, A. M. Kelleher, C. Ranjit, D. J. Schust, T. E. Spencer, Basolateral secretions of human endometrial epithelial organoids impact stromal cell decidualization. *Mol Hum Reprod* **29** (2023).
18. P. M. Kirkwood *et al.*, Single-cell RNA sequencing and lineage tracing confirm

mesenchyme to epithelial transformation (MET) contributes to repair of the endometrium at menstruation. *Elife* **11** (2022).

19. S. G. Paule *et al.*, Podocalyxin is a key negative regulator of human endometrial epithelial receptivity for embryo implantation. *Hum Reprod* **36**, 1353-1366 (2021).
20. R. S. Auriemma *et al.*, The Interplay Between Prolactin and Reproductive System: Focus on Uterine Pathophysiology. *Front Endocrinol (Lausanne)* **11**, 594370 (2020).
21. S. P. d'Hauterive *et al.*, Human Chorionic Gonadotropin and Early Embryogenesis: Review. *Int J Mol Sci* **23** (2022).
22. C. Nwabuobi *et al.*, hCG: Biological Functions and Clinical Applications. *Int J Mol Sci* **18** (2017).
23. F. W. Bazer, R. C. Burghardt, G. A. Johnson, T. E. Spencer, G. Wu, Mechanisms for the establishment and maintenance of pregnancy: synergies from scientific collaborations. *Biol Reprod* **99**, 225-241 (2018).
24. L. Garcia-Alonso *et al.*, Mapping the temporal and spatial dynamics of the human endometrium in vivo and in vitro. *Nat Genet* **53**, 1698-1711 (2021).
25. L. E. K. Rocío Martínez-Aguilar, Jane J Reavey, Hilary O D Critchley and Jacqueline A Maybin, HYPOXIA AND REPRODUCTIVE HEALTH: The presence and role of hypoxia in the endometrium. *Reproduction* 10.1530/rep, F1-F17 (2021).
26. M. Fatmous, A. Rai, Q. H. Poh, L. A. Salamonsen, D. W. Greening, Endometrial small extracellular vesicles regulate human trophectodermal cell invasion by reprogramming the phosphoproteome landscape. *Front Cell Dev Biol* **10**, 1078096 (2022).
27. X. Jiang *et al.*, Lack of VMP1 impairs hepatic lipoprotein secretion and promotes non-alcoholic steatohepatitis. *J Hepatol* **77**, 619-631 (2022).
28. W. T. Kuo *et al.*, The Tight Junction Protein ZO-1 Is Dispensable for Barrier Function but Critical for Effective Mucosal Repair. *Gastroenterology* **161**, 1924-1939 (2021).
29. L. Bissonnette *et al.*, Human S100A10 plays a crucial role in the acquisition of the endometrial receptivity phenotype. *Cell Adh Migr* **10**, 282-298 (2016).
30. C. Srivastava *et al.*, FAT1 modulates EMT and stemness genes expression in hypoxic glioblastoma. *Int J Cancer* **142**, 805-812 (2018).
31. L. Liu *et al.*, si-SNHG5-FOXF2 inhibits TGF-beta1-induced fibrosis in human primary endometrial stromal cells by the Wnt/beta-catenin signalling pathway. *Stem Cell Res Ther* **11**, 479 (2020).
32. J. Geng, C. Cui, Y. Yin, Y. Zhao, C. Zhang, LncRNA NEAT1 affects endometrial receptivity by regulating HOXA10 promoter activity. *Cell Cycle* **21**, 1932-1944 (2022).
33. M. F. Vargas *et al.*, Effect of single post-ovulatory administration of levonorgestrel on gene expression profile during the receptive period of the human endometrium. *J Mol Endocrinol* **48**, 25-36 (2012).
34. S. Kinnear, L. A. Salamonsen, M. Francois, V. Harley, J. Evans, Uterine SOX17: a key player in human endometrial receptivity and embryo implantation. *Sci Rep* **9**, 15495 (2019).
35. P. Huang *et al.*, SOX4 facilitates PGR protein stability and FOXO1 expression conducive for human endometrial decidualization *Elife* **2022 Mar 4;11:e72073.** (2021).
36. A. He *et al.*, The role of transcriptomic biomarkers of endometrial receptivity in personalized embryo transfer for patients with repeated implantation failure. *J Transl Med* **19**, 176 (2021).

37. A. Devesa-Peiro, P. Sebastian-Leon, A. Parraga-Leo, A. Pellicer, P. Diaz-Gimeno, Breaking the ageing paradigm in endometrium: endometrial gene expression related to cilia and ageing hallmarks in women over 35 years. *Hum Reprod* **37**, 762-776 (2022).
38. K. Kalra, J. Eberhard, N. Farbehi, J. J. Chong, M. Xaymardan, Role of PDGF-A/B Ligands in Cardiac Repair After Myocardial Infarction. *Front Cell Dev Biol* **9**, 669188 (2021).
39. Y. Yang *et al.*, SLC25A1 promotes tumor growth and survival by reprogramming energy metabolism in colorectal cancer. *Cell Death Dis* **12**, 1108 (2021).
40. M. N. Lasse D. Jensen, et al, VEGF-B-Neuropilin-1 signaling is spatiotemporally indispensable for vascular and neuronal development in zebrafish. *PNAS* **Nov 3** (2015).
41. M. Li *et al.*, BUB1 Is Identified as a Potential Therapeutic Target for Pancreatic Cancer Treatment. *Front Public Health* **10**, 900853 (2022).
42. T. Li *et al.*, WNT5A Interacts With FZD5 and LRP5 to Regulate Proliferation and Self-Renewal of Endometrial Mesenchymal Stem-Like Cells. *Front Cell Dev Biol* **10**, 837827 (2022).
43. A. Owusu-Akyaw, K. Krishnamoorthy, L. T. Goldsmith, S. S. Morelli, The role of mesenchymal-epithelial transition in endometrial function. *Hum Reprod Update* **25**, 114-133 (2019).
44. A. Casazza *et al.*, Impeding macrophage entry into hypoxic tumor areas by Sema3A/Nrp1 signaling blockade inhibits angiogenesis and restores antitumor immunity. *Cancer Cell* **24**, 695-709 (2013).
45. X. Wang *et al.*, Functional role of arginine during the peri-implantation period of pregnancy. I. Consequences of loss of function of arginine transporter SLC7A1 mRNA in ovine conceptus trophectoderm. *FASEB J* **28**, 2852-2863 (2014).
46. S. A. Robertson, P. Y. Chin, J. G. Femia, H. M. Brown, Embryotoxic cytokines-Potential roles in embryo loss and fetal programming. *J Reprod Immunol* **125**, 80-88 (2018).
47. L. Du *et al.*, Single-cell transcriptome analysis reveals defective decidua stromal niche attributes to recurrent spontaneous abortion. *Cell Prolif* **54**, e13125 (2021).
48. C. Sancakli Usta, G. Turan, C. B. Bulbul, A. Usta, E. Adali, Differential expression of Oct-4, CD44, and E-cadherin in eutopic and ectopic endometrium in ovarian endometriomas and their correlations with clinicopathological variables. *Reprod Biol Endocrinol* **18**, 116 (2020).
49. G. Le Friec *et al.*, The CD46-Jagged1 interaction is critical for human TH1 immunity. *Nat Immunol* **13**, 1213-1221 (2012).
50. A. P. Bielfeld *et al.*, A Proteome Approach Reveals Differences between Fertile Women and Patients with Repeated Implantation Failure on Endometrial Level(-)Does hCG Render the Endometrium of RIF Patients? *Int J Mol Sci* **20** (2019).
51. X. W. Gu *et al.*, ATP mediates the interaction between human blastocyst and endometrium. *Cell Prolif* **53**, e12737 (2020).
52. K. King *et al.*, Dynamics of lipid droplets in the endometrium and fatty acids and oxylipins in the uterine lumen, blood, and milk of lactating cows during diestrus. *J Dairy Sci* **104**, 3676-3692 (2021).
53. F. Vilella, L. B. Ramirez, C. Simon, Lipidomics as an emerging tool to predict endometrial receptivity. *Fertil Steril* **99**, 1100-1106 (2013).
54. D. Braga *et al.*, Lipidomic profile as a noninvasive tool to predict endometrial receptivity.

Mol Reprod Dev **86**, 145-155 (2019).

55. S. Guo *et al.*, Hypoxia and its possible relationship with endometrial receptivity in adenomyosis: a preliminary study. *Reprod Biol Endocrinol* **19**, 7 (2021).

56. M. Chen *et al.*, Bioinformatic analysis reveals the importance of epithelial-mesenchymal transition in the development of endometriosis. *Sci Rep* **10**, 8442 (2020).

57. N. Gjorevski *et al.*, Tissue geometry drives deterministic organoid patterning. *Science* **375**, eaaw9021 (2022).

Fig 1 Endometrial organoids possess endometrial morphology and function

(A) Human endometrial organoids constructed from adult stem cells were treated with expansion medium (ExM) (CTRL) or subjected to hormonal stimulation. Timeline of endometrial organoid cultured by ExM (CTRL), ovarian steroid hormones simulating secretory phase (SEC), ovarian steroid hormones combining PRL and placental hormones to mimic the window of implantation (WOI).

(B) Endometrial organoids in the CTRL, SEC and WOI groups displayed similar growth patterns during the culture period. Scale bar = 200 μm.

(C) Screenshot of video S1 showing endometrial glands gradually developing into a vesicular shape, and the surrounding stromal cells arranging in a fibrous pattern in the CTRL endometrial organoids (100x, up-left). Screenshot of video S2 displaying the stromal cells growing in fibrous pattern and forming an extensive network in the CTRL endometrial organoids (200x, up-right). (The yellow arrows indicate stromal cells and the white arrows indicate endometrial glands). The epithelial cells arrange like paving stones (middle and down, left). Stromal cells formed an extensive network (middle and down, right). The arrowhead indicates stromal cells. Scale bar = 100 μm (middle), Scale bar = 50 μm (down).

(D) Validation of epithelial, stromal cell and endometrial gland markers (E-cadherin, vimentin and FOXA2, respectively) with immunofluorescence (IF) in the endometrium in vivo and CTRL endometrial organoids in vitro. Nuclei were counterstained with DAPI. Scale bar = 40 μm. Periodic acid-schiff staining (PAS) of endometrium in vivo and endometrial organoid in vitro. Scale bar = 20 μm.

(E) IF analysis of proliferation and apoptosis indicated by Ki67 and cleaved caspase-3 in the CTRL organoids, respectively. Nuclei were counterstained with DAPI. Scale bar = 40 μm.

Fig 2 Developing receptive endometrial organoids in vitro mimicking the implantation-window endometrium

(A) T-SNE plot of scRNA-seq data from three individual endometrial organoids of the CTRL, SEC and WOI groups (left). T-SNE plot of combined scRNA-seq data from the three kinds of organoids and mid-secretory endometrium (right).

(B) Exhibition of stromal cell marked by vimentin of CTRL organoid through whole-mount clearing, immunostaining and light sheet microscopy imaging. Nuclei were counterstained with DAPI. The arrowhead indicates stromal cells. Scale bar = 40 μm (left), Scale bar = 30 μm (right).

(C) Exhibition of immune cell marked by CD45 and CD44, and endometrial gland marked by FOXA2 of CTRL organoid through whole-mount clearing, immunostaining and light sheet microscopy imaging. Nuclei were counterstained with DAPI. The arrowhead indicates immune cells. Scale bar = 50 μm (left), Scale bar = 10 μm (right).

(D) Flow cytometric analysis of T cells and macrophages in the CTRL endometrial organoid. Gating strategy used for determining white blood cells (WBC) ($CD45^+$ cells), T cells ($CD45^+CD3^+$ cells) and macrophages ($CD45^+CD68^+CD11b^+$ cells).

(E) Heatmap and bubble diagram illustrating highly expressed genes as well as GO functions enriched in both organoids during the WOI and mid secretory endometrial tissue in terms of SOX9+LGR5+ epithelium, stem-derived epithelium, secretory epithelium, proliferative epithelium, unciliated epithelium, stromal cells and EMT-derived stromal cells. The color of heatmap represents log-transformed fold change of gene expression.

(F) Heatmaps showing differentially expressed TFs of endometrial organoids and endometrium in the secretory epithelium (left) and EMT-derived stromal cells (right). The color represents log-transformed fold change of gene expression.

(G) Endometrial receptivity evaluation of endometrium and their derived WOI organoids through ERT. Asterisks indicate individual samples.

(H) Electron micrograph of the CTRL (top), SEC (middle) and WOI (bottom) endometrial organoid showing pinopodes (P), glycogen granule (asterisk), microvilli (white arrows) and cilia (orange arrows). Scale bar = 1 μm. Quantitative comparison of pinopodes, glycogen, microvilli, and cilia in the CTRL, SEC and WOI organoids. *$P \leq 0.05$, **$P \leq 0.005$, ***$P \leq 0.0005$, ****$P \leq 0.0001$.

Fig 3 Receptive endometrial organoid exhibits the implantation window at the transcription and protein levels

(A) Principal component analysis (PCA) plot computed with differentially expressed genes in the bulk transcriptome of endometrial organoids belonging to the CTRL, SEC and WOI groups.

(B) Heatmap showing that enrichment of differentially expressed genes for the terms of extracellular matrix remodeling, hormone response, negative regulation of cell proliferation, monocarboxylic acid metabolism, lipid metabolism, cell adhesion, negative regulation of cell differentiation and RHO GTPase signaling. The color represents log-transformed fold change of gene expression.

(C) Responsiveness to progesterone and estrogen was evaluated by IF to PRA/B and OLFM4 with IF respectively. Scale bar = 40 μm, $^{**}P \leq 0.005$.

(D) Exhibition of implantation marker (FOXO1) and endometrial gland marker (FOXA2) through combination of organoid clearing, IF and light sheet microscopy. Nuclei were counterstained with DAPI. $^{**}P \leq 0.005$.

(E) PCA plot computed with differentially expressed proteins in the microproteomics of endometrial organoids belonging to the CTRL, SEC and WOI groups.

(F) Dot bar diagram exhibiting protein expression levels related to cilia in the CTRL and WOI groups (left). Dot bar diagram displaying tubulin, integrin and PI3K-AKT pathway-related protein expression levels in the SEC and WOI groups (right).

(G) IF analysis of cilia assembly marked by acetyl-α-tubulin. Nuclei were counterstained with DAPI. The arrowhead indicates cilia. Scale bar = 50 μm. $^{*}P \leq 0.05$.

Fig 4 Receptive endometrial organoid exhibits the implantation window at single cell level

(A) Bar graph exhibiting various percentages of each cell type in the three groups.

(B) Gene set enrichment analysis (GSEA) between the SEC and WOI groups for the secretory epithelium.

(C-E) Pseudotime trajectory showing the transformation between proliferative and secretory epithelium (C), ciliated and unciliated epithelium (D), proliferative epithelium and EMT-derived stromal cells (E) in the CTRL, SEC and WOI groups. Arrows indicate the direction of the pseudotime trajectory.

(F-G) Dot plots demonstrating the Cellphone DB analysis of relevant receptors and ligands of ciliated epithelium (F) and EMT-derived stromal cells (G) with other cell types. The size of the dot represents the level of significance. The color of the dot indicates the mean of the average expression level of interacting molecule 1 in ciliated epithelium or EMT-derived stromal cells and molecule 2 in other cell types.

Fig.5 Schematic diagram displaying the establishment and validation of receptive endometrial organoids, and summarizing the characteristic biological events of implantation-window endometrium.

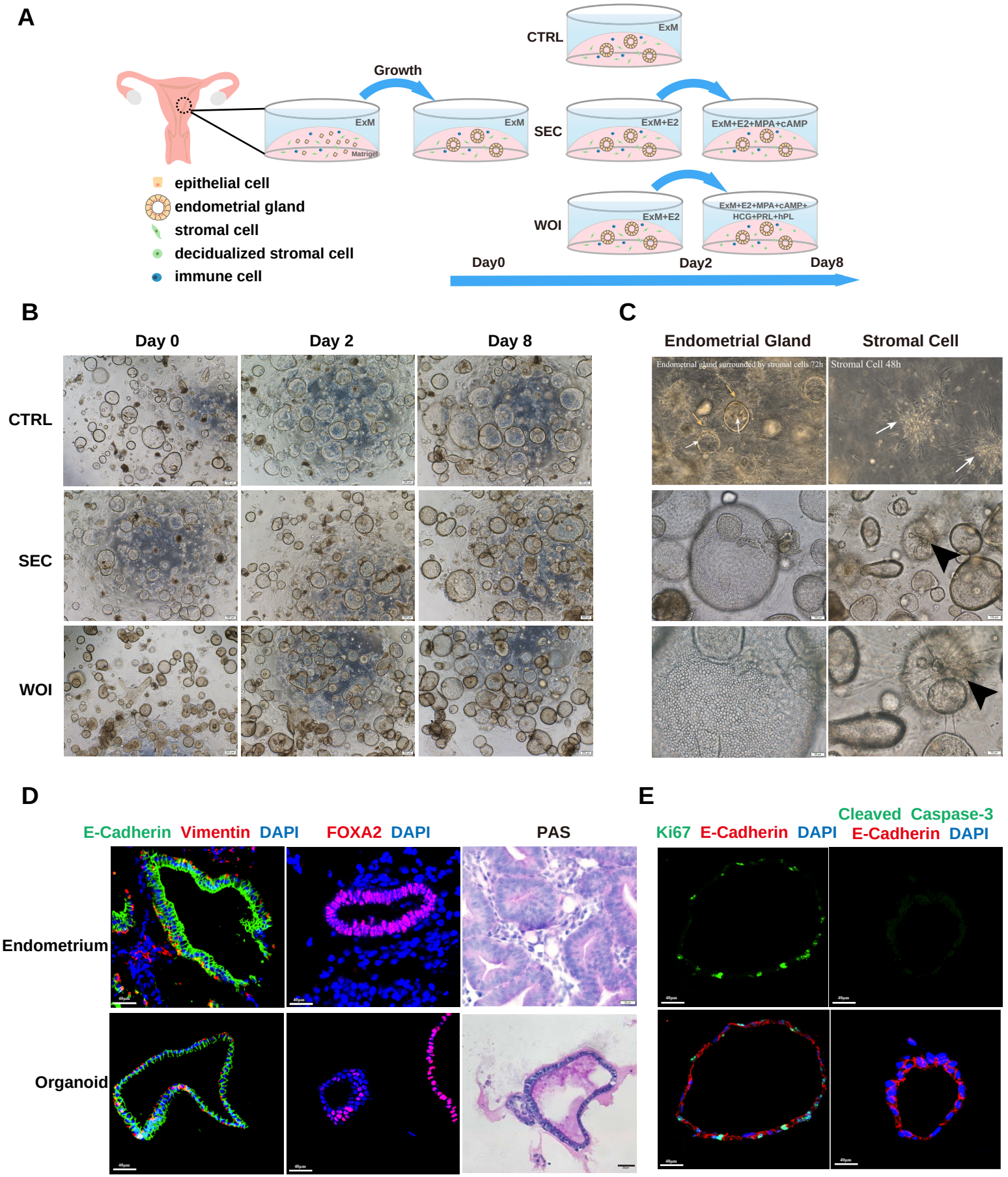
A
CTRL
ExM
Growth
ExM
Matrigel
ExM
SEC
ExM+E2
ExM+E2+MPA+cAMP
WOI
ExM+E2
ExM+E2+MPA+cAMP+
HCG+PRL+hPL
epithelial cell
endometrial gland
stromal cell
decidualized stromal cell
immune cell
Day0
Day2
Day8
B
Day 0
Day 2
Day 8
CTRL
SEC
WOI
C
Endometrial Gland
Stromal Cell
Endometrial gland surrounded by stromal cells 72h
Stromal Cell 48h
D
E-Cadherin Vimentin DAPI
FOXA2 DAPI
PAS
Endometrium
Organoid
E
Ki67 E-Cadherin DAPI
Cleaved Caspase-3
E-Cadherin DAPI

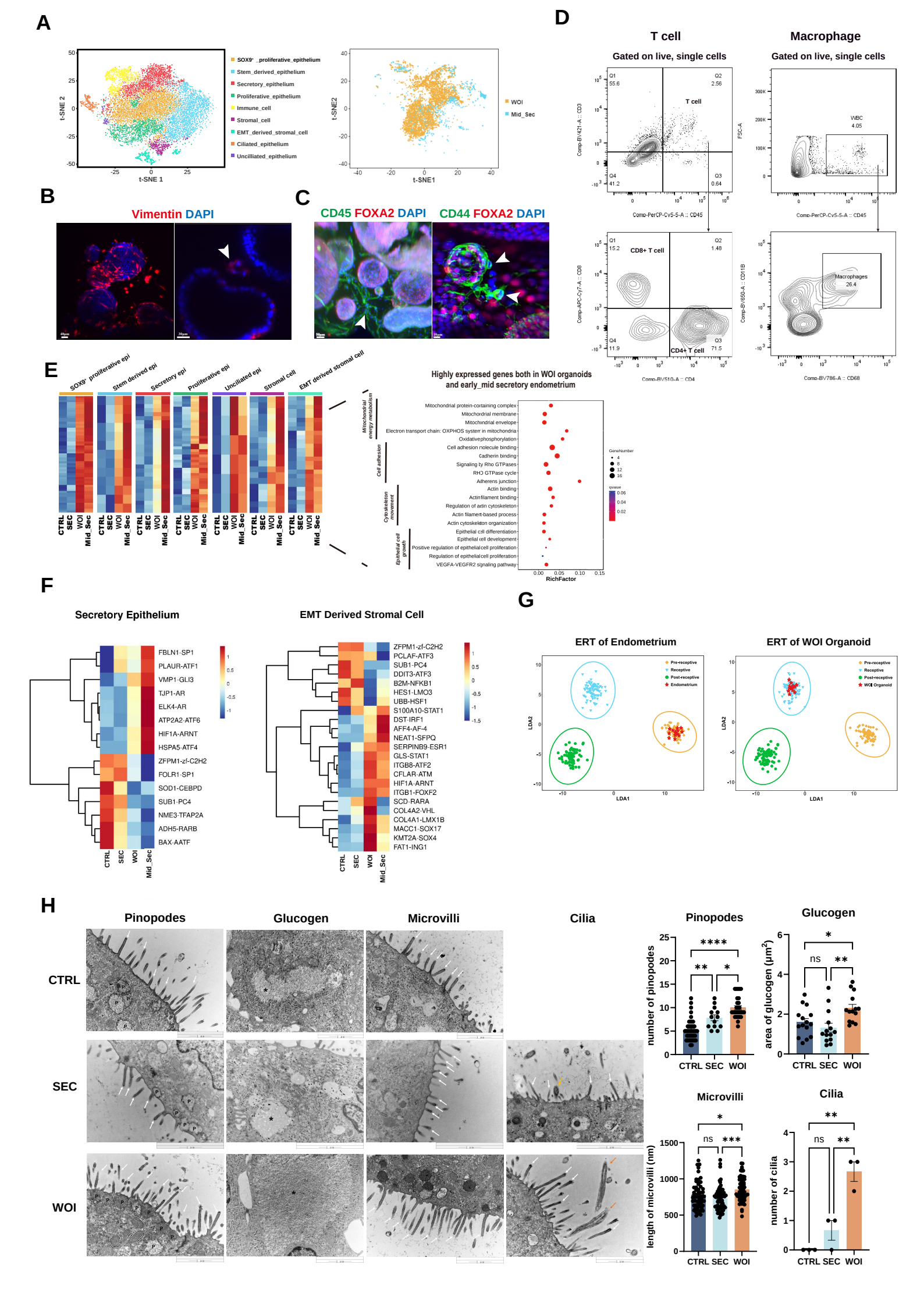
A
t-SNE 1
t-SNE 2
SOX9+ _proliferative_epithelium
Stem_derived_epithelium
Secretory_epithelium
Proliferative_epithelium
Immune_cell
Stromal_cell
EMT_derived_stromal_cell
Ciliated_epithelium
Uncilliated_epithelium
t-SNE1
t-SNE2
WOI
Mid_Sec
B
Vimentin DAPI
C
CD45 FOXA2 DAPI
CD44 FOXA2 DAPI
D
T cell
Macrophage
Gated on live, single cells
Gated on live, single cells
T cell
CD8+ T cell
CD4+ T cell
WBC
Macrophages
E
SOX9+ proliferative epi
Stem derived epi
Secretory epi
Proliferative epi
Unciliated epi
Stromal cell
EMT derived stromal cell
CTRL
SEC
WOI
Mid_Sec
Highly expressed genes both in WOI organoids and early_mid secretory endometrium
Mitochondrial energy metabolism
Cell adhesion
Cytoskeleton movement
Epithelial cell growth
Mitochondrial protein-containing complex
Mitochondrial membrane
Mitochondrial envelope
Electron transport chain: OXPHOS system in mitochondria
Oxidative phosphorylation
Cell adhesion molecule binding
Cadherin binding
Signaling by Rho GTPases
RHO GTPase cycle
Adherens junction
Actin binding
Actin filament binding
Regulation of actin cytoskeleton
Actin filament-based process
Actin cytoskeleton organization
Epithelial cell differentiation
Epithelial cell development
Positive regulation of epithelial cell proliferation
Regulation of epithelial cell proliferation
VEGFA-VEGFR2 signaling pathway
RichFactor
GeneNumber
F
Secretory Epithelium
EMT Derived Stromal Cell
FBLN1-SP1
PLAUR-ATF1
VMP1-GLI3
TJP1-AR
ELK4-AR
ATP2A2-ATF6
HIF1A-ARNT
HSPA5-ATF4
ZFPM1-zf-C2H2
FOLR1-SP1
SOD1-CEBPD
SUB1-PC4
NME3-TFAP2A
ADH5-RARB
BAX-AATF
ZFPM1-zf-C2H2
PCLAF-ATF3
SUB1-PC4
DDIT3-ATF3
B2M-NFKB1
HES1-LMO3
UBB-HSF1
S100A10-STAT1
DST-IRF1
AFF4-AF-4
NEAT1-SFPQ
SERPINB9-ESR1
GLS-STAT1
ITGB8-ATF2
CFLAR-ATM
HIF1A-ARNT
ITGB1-FOXF2
SCD-RARA
COL4A2-VHL
COL4A1-LMX1B
MACC1-SOX17
KMT2A-SOX4
FAT1-ING1
G
ERT of Endometrium
ERT of WOI Organoid
Pre-receptive
Receptive
Post-receptive
Endometrium
WOI Organoid
LDA1
LDA2
H
Pinopodes
Glucogen
Microvilli
Cilia
CTRL
SEC
WOI
number of pinopodes
area of glucogen (μm²)
length of microvilli (nm)
number of cilia
ns

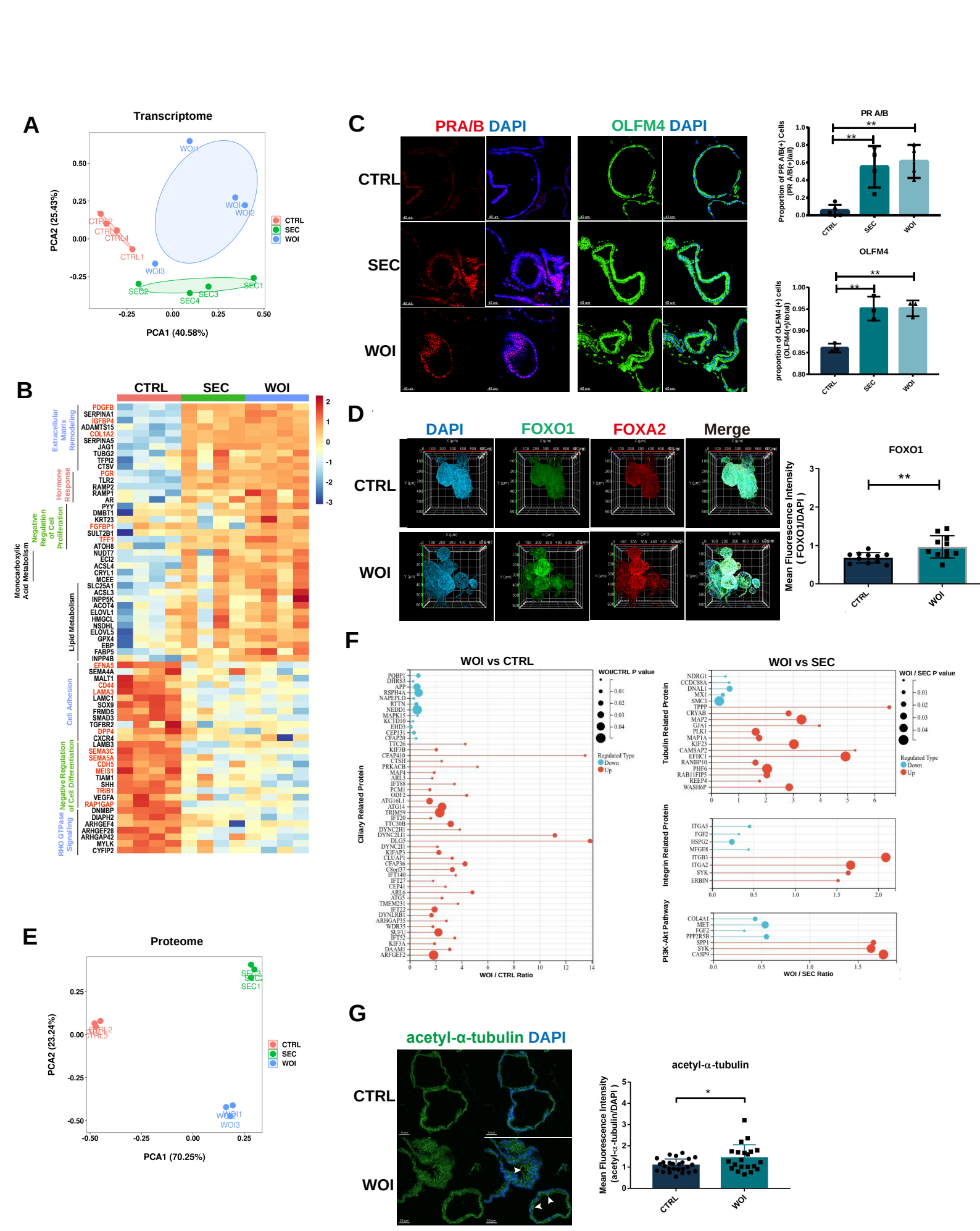
A
Transcriptome
PCA2 (25.43%)
PCA1 (40.58%)
CTRL
SEC
WOI
B
CTRL
SEC
WOI
Extracellular Matrix Remodeling
Hormone Response
Negative Regulation of Cell Proliferation
Monocarboxylic Acid Metabolism
Lipid Metabolism
Cell Adhesion
Negative Regulation of Cell Differentiation
RHO GTPase Signalling
C
PRA/B DAPI
OLFM4 DAPI
CTRL
SEC
WOI
PR A/B
Proportion of PR A/B(+) Cells (PR A/B(+)/all)
OLFM4
proportion of OLFM4 (+) cells (OLFM4(+)/total)
D
DAPI
FOXO1
FOXA2
Merge
CTRL
WOI
FOXO1
Mean Fluorescence Intensity (FOXO1/DAPI)
E
Proteome
PCA2 (23.24%)
PCA1 (70.25%)
CTRL
SEC
WOI
F
WOI vs CTRL
WOI vs SEC
WOI/CTRL P value
WOI / SEC P value
Regulated Type
Down
Up
Ciliary Related Protein
Tubulin Related Protein
Integrin Related Protein
PI3K-Akt Pathway
WOI / CTRL Ratio
WOI / SEC Ratio
G
acetyl-α-tubulin DAPI
CTRL
WOI
acetyl-α-tubulin
Mean Fluorescence Intensity (acetyl-α-tubulin/DAPI)

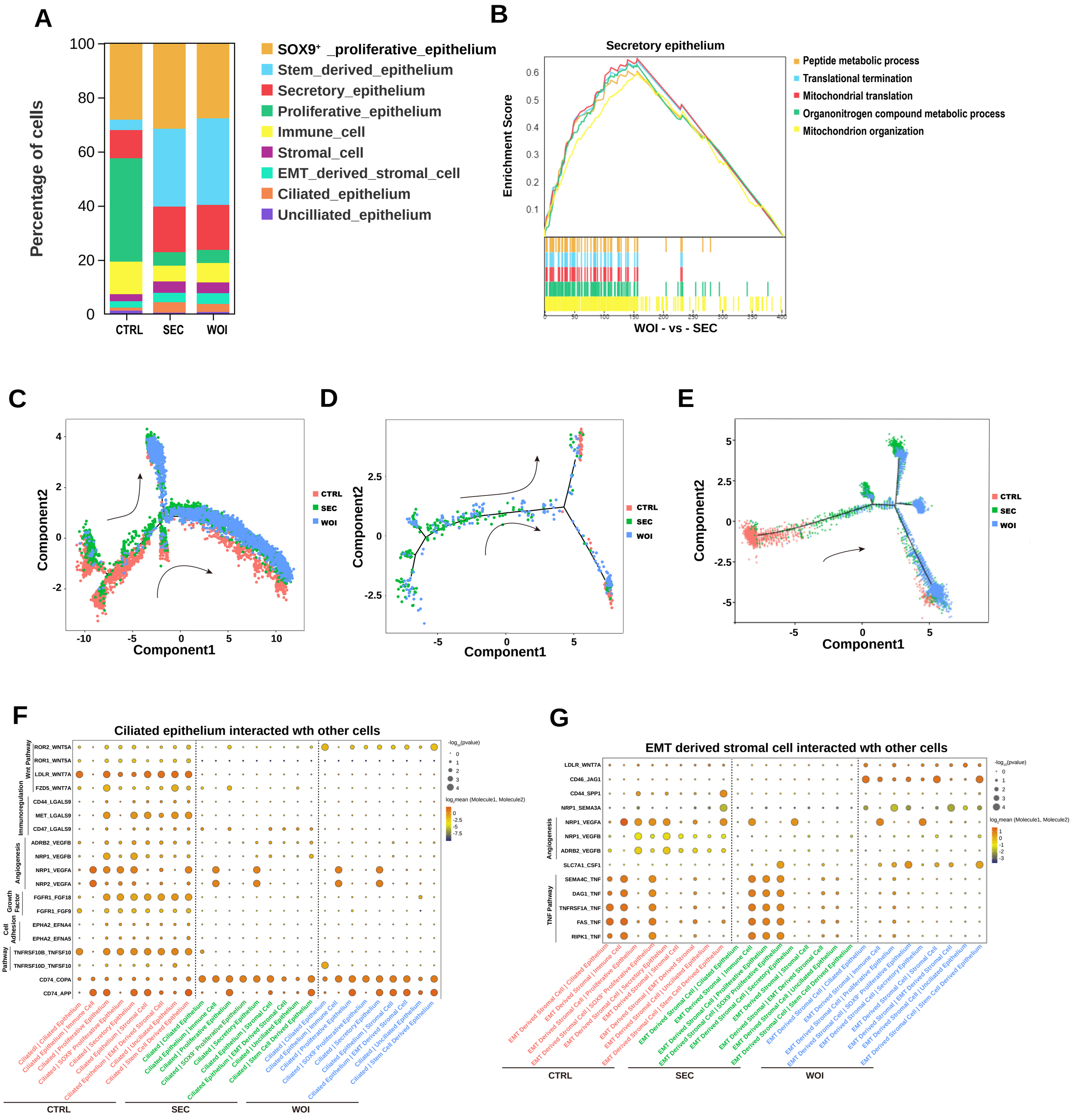
A
Percentage of cells
CTRL
SEC
WOI
SOX9+ _proliferative_epithelium
Stem_derived_epithelium
Secretory_epithelium
Proliferative_epithelium
Immune_cell
Stromal_cell
EMT_derived_stromal_cell
Ciliated_epithelium
Uncilliated_epithelium
B
Secretory epithelium
Enrichment Score
Peptide metabolic process
Translational termination
Mitochondrial translation
Organonitrogen compound metabolic process
Mitochondrion organization
WOI - vs - SEC
C
Component1
Component2
D
E
F
Ciliated epithelium interacted wth other cells
Wnt Pathway
Immunoregulation
Angiogenesis
Growth Factor
Cell Adhesion
TNF Pathway
ROR2_WNT5A
ROR1_WNT5A
LDLR_WNT7A
FZD5_WNT7A
CD44_LGALS9
MET_LGALS9
CD47_LGALS9
ADRB2_VEGFB
NRP1_VEGFB
NRP1_VEGFA
NRP2_VEGFA
FGFR1_FGF18
FGFR1_FGF9
EPHA2_EFNA4
EPHA2_EFNA5
TNFRSF10B_TNFSF10
TNFRSF10D_TNFSF10
CD74_COPA
CD74_APP
G
EMT derived stromal cell interacted wth other cells
LDLR_WNT7A
CD46_JAG1
CD44_SPP1
NRP1_SEMA3A
NRP1_VEGFA
NRP1_VEGFB
ADRB2_VEGFB
SLC7A1_CSF1
SEMA4C_TNF
DAG1_TNF
TNFRSF1A_TNF
FAS_TNF
RIPK1_TNF
CTRL
SEC
WOI

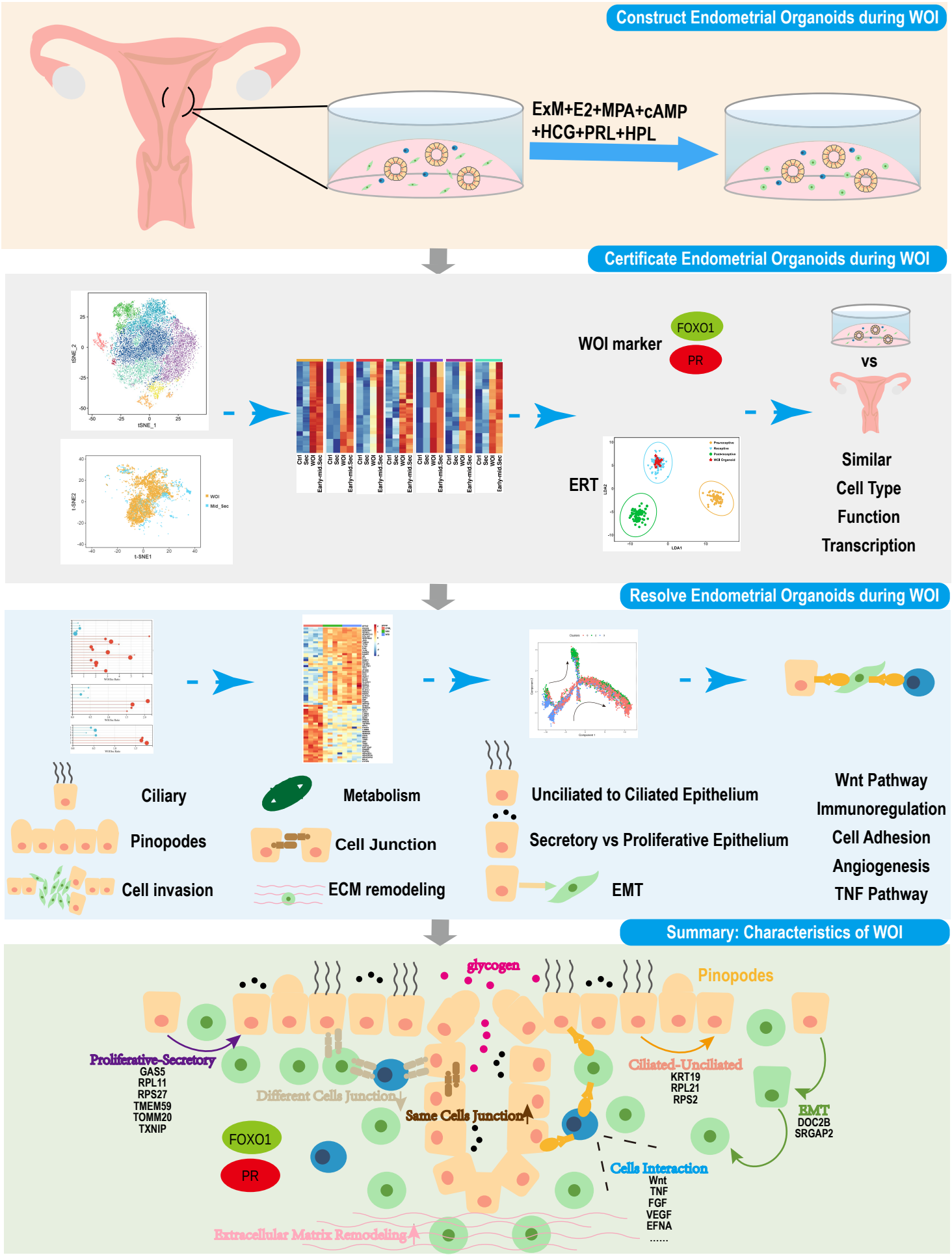
Construct Endometrial Organoids during WOI
ExM+E2+MPA+cAMP
+HCG+PRL+HPL
Certificate Endometrial Organoids during WOI
WOI marker
FOXO1
PR
ERT
vs
Similar
Cell Type
Function
Transcription
Resolve Endometrial Organoids during WOI
Ciliary
Pinopodes
Cell invasion
Metabolism
Cell Junction
ECM remodeling
Unciliated to Ciliated Epithelium
Secretory vs Proliferative Epithelium
EMT
Wnt Pathway
Immunoregulation
Cell Adhesion
Angiogenesis
TNF Pathway
Summary: Characteristics of WOI
glycogen
Pinopodes
Proliferative-Secretory
GAS5
RPL11
RPS27
TMEM59
TOMM20
TXNIP
Different Cells Junction
Same Cells Junction
Ciliated-Unciliated
KRT19
RPL21
RPS2
EMT
DOC2B
SRGAP2
FOXO1
PR
Cells Interaction
Wnt
TNF
FGF
VEGF
EFNA
.....
Extracellular Matrix Remodeling